Molecules and Cells

An Essential Role of the N-Terminal Region of ACSL1 in Linking Free Fatty Acids to Mitochondrial β-Oxidation in C2C12 Myotubes

Jinyan Nan[1], Ji Seon Lee[1], Seung-Ah Lee[2], Dong-Sup Lee[1], Kyong Soo Park[3,4], and Sung Soo Chung[5,*]

[1]Department of Biomedical Sciences, Seoul National University College of Medicine, Seoul 03080, Korea, [2]Genomic Medicine Institute, Seoul National University Medical Research Center, Seoul 03080, Korea, [3]Department of Internal Medicine, Seoul National University College of Medicine, Seoul 03080, Korea, [4]Department of Molecular Medicine and Biopharmaceutical Sciences, Graduate School of Convergence Science and Technology, Seoul National University College of Medicine, Seoul 03080, Korea, [5]Biomedical Research Institute, Seoul National University Hospital, Seoul 03080, Korea
*Correspondence: suschung@snu.ac.kr
https://doi.org/10.14348/molcells.2021.0077
www.molcells.org

Free fatty acids are converted to acyl-CoA by long-chain acyl-CoA synthetases (ACSLs) before entering into metabolic pathways for lipid biosynthesis or degradation. ACSL family members have highly conserved amino acid sequences except for their N-terminal regions. Several reports have shown that ACSL1, among the ACSLs, is located in mitochondria and mainly leads fatty acids to the β-oxidation pathway in various cell types. In this study, we investigated how ACSL1 was localized in mitochondria and whether ACSL1 overexpression affected fatty acid oxidation (FAO) rates in C2C12 myotubes. We generated an ACSL1 mutant in which the N-terminal 100 amino acids were deleted and compared its localization and function with those of the ACSL1 wild type. We found that ACSL1 adjoined the outer membrane of mitochondria through interaction of its N-terminal region with carnitine palmitoyltransferase-1b (CPT1b) in C2C12 myotubes. In addition, overexpressed ACSL1, but not the ACSL1 mutant, increased FAO, and ameliorated palmitate-induced insulin resistance in C2C12 myotubes. These results suggested that targeting of ACSL1 to mitochondria is essential in increasing FAO in myotubes, which can reduce insulin resistance in obesity and related metabolic disorders.

Keywords: ACSL1, fatty acid oxidation, insulin resistance, mitochondria, myotubes

INTRODUCTION

Depending on fuel availability, skeletal muscle can use both glucose and fatty acids for energy (Kelley and Mandarino, 2000). Increased serum free fatty acids in energy excess state like obesity causes lipid accumulation in the peripheral tissues, such as skeletal muscle and liver, which results in insulin resistance (Badin et al., 2013; Czech, 2017; Koves et al., 2008). Excess intracellular palmitate is converted to diacylglycerol (DAG) and ceramide, two major inducers of insulin resistance (Chaurasia and Summers, 2015; Coll et al., 2008; Palomer et al., 2018). Several reports have shown that increased fatty acid oxidation (FAO) reduces cellular DAG and ceramide levels and restores the insulin signaling pathway (Bruce et al., 2009; Henique et al., 2010; Sebastian et al., 2007). Therefore, enhancing FAO is a potential therapeutic treatment for obesity-induced insulin resistance.

Free fatty acids must be converted to acyl-CoAs by a long-chain acyl-CoA synthetase (ACSL) family member before

Received 8 April, 2021; revised 15 July, 2021; accepted 3 August, 2021; published online 13 September, 2021

eISSN: 0219-1032

entering into the synthetic pathways of cholesterol esters, phospholipids, DAG, and triacylglycerol (TG) or into the β oxidation pathway (Soupene and Kuypers, 2008). ACSL isoforms have different tissue distributions, subcellular localizations and nutrient responses (Mashek et al., 2006). It has been thought that ACSL isoforms are localized at various intracellular membranes, such as the plasma, endoplasmic reticulum (ER), mitochondria, and microsomal membranes, and their active sites face the cytoplasm (Gargiulo et al., 1999; Mannaerts et al., 1982). In addition, several studies reported that the fate of an acyl-CoA toward β-oxidation or lipid biosynthesis was determined by the ACSL isoform-mediated compartmentalization of acyl-CoA (Bowman et al., 2016; Bu et al., 2009; Cooper et al., 2015; Ellis et al., 2010; Li et al., 2015; Teodoro et al., 2017). ACSL1, one of the ACSL family members, mainly directs fatty acids toward β-oxidation. ACSL1 deficiency decreases FAO in skeletal muscle, cardiac muscle, and adipose tissues (Ellis et al., 2010; Grevengoed et al., 2015; Zhao et al., 2019). However, other reports showed that ACSL1 was also located on the ER as well as mitochondria in the liver, and many proteins in the mitochondria and ER were identified as ACSL1 interacting proteins in hepatocytes by proteomics analyses (Li et al., 2009; Young et al., 2018). Liver-specific knockout of *Acsl1* reduced TG contents and FAO, as well as changing the phospholipid composition (Li et al., 2009). However, ACSL1 overexpression in liver or hepatocytes increases TG and phospholipids, with targeting of the overexpressed ACSL1 to the ER (Li et al., 2006; Parkes et al., 2006). These results suggest that the localization of ACSL1 in mitochondria is important for FAO.

We previously showed that the transcript levels of carnitine palmitoyltransferase-1b (CPT1b), a master regulator of FAO rates, and ACSL1 were increased by treatment with high levels of palmitate in skeletal myotubes, which was mediated by activation of peroxisome proliferator-activated receptor δ (PPARδ) and PPARγ through desumoylation (Koo et al., 2015). Consistently, SUMO-specific protease 2 overexpression in skeletal muscle protected mice from high fat diet-induced obesity and insulin resistance by increasing FAO through upregulation of CPT1b and ACSL1 expressions (Koo et al., 2015). We therefore hypothesized that ACSL1 overexpression in myotubes facilitated FAO, unlike the effect of ACSL1 overexpression in the liver. In addition, we also hypothesized that the N-terminal region of ACSL1 was important for its localization to mitochondria. ACSL family members have highly conserved amino acid sequences except for their N-terminal regions of approximately 100 amino acids. The N-terminal regions of ACSL isoforms contain predicted transmembrane spanning segments (for example, amino acids from 25 to 45 of ACSL1) (Soupene and Kuypers, 2006).

In this study, we constructed an N-terminal 100 amino acid-deletion mutant of ACSL1, and investigated its cellular location and function compared with the wild type form of ACSL1. Unlike the wild type, the ACSL1 mutant is not located in mitochondria. In addition, overexpression of ACSL1 wild type, but not the ACSL1 mutant, increased FAO in C2C12 myotubes.

MATERIALS AND METHODS

Cell culture

COS7 cells were maintained in Dulbecco's modified Eagle's medium (DMEM) supplemented with 10% fetal bovine serum (FBS) in a 5% CO_2 incubator. C2C12 myoblasts were maintained in DMEM supplemented with 10% FBS. Differentiation to myotubes was induced by incubation with DMEM containing 2% horse serum (Invitrogen, USA) for 4-7 days.

Transfection of plasmids, virus infection, and siRNA treatment

An expression vector for the wild type form of ACSL1 (pcDNA-HA-ACSL1wt) was constructed by sub-cloning the full-length of a mouse ACSL1 cDNA fragment into the pcDNA-HA vector. The expression vector of an ACSL1 mutant form (pcDNA-HA-ACSL1mt) was generated by inserting an ACSL1 cDNA fragment lacking the N-terminal 100 amino acids to pcDNA-HA. The pCMV-mCPT1b-Myc was purchased from Sino Biological (China). Plasmid transfection was performed using Lipofectamine with Plus Reagent (Invitrogen). Specific siRNAs against ACSL1, ACSL3, and CPT1b were purchased from Dhamarcon (USA), and the siRNAs (50 nmol/L) were transfected using RNAiMAX (Invitrogen). To generate the adenovirus expressing Ad-HA-ACSL1wt or Ad-HA-ACSL1mt, the DNA fragments coding HA-ACSL1 cDNA were inserted into pAdTrack-CMV, followed by recombination with pAdEasy. Ad-HA-ACSL1 was generated by transfecting the recombinant adenoviral DNA into AD-293 cells. C2C12 myotubes were infected with Ad-GFP (control), Ad-ACSL1wt or Ad-ACSL1mt (100 moi) for 24 h.

Immunofluorescence

C2C12 myotubes, COS7 or HepG2 cells were incubated with 100 nmol/L Mito-Tracker (Thermo Fisher Scientific, USA) or 1 μmol/L ER-Tracker (Thermo Fisher Scientific) for 30 min, followed by fixation in 4% paraformaldehyde for 10 min, then washing three times with phosphate-buffered saline (PBS). Cells were treated with 0.25% Triton X-100 in PBS for 10 min, followed by three washes with PBS. After incubation with 5% normal goat serum in PBS for 1 h, the cells were incubated with an antibody against HA (1:500 in 2.5% normal goat serum; Santa Cruz Biotechnology, USA) at 4°C overnight. On the following day, the cells were washed with PBS four times and treated with Alexa 568-conjugated secondary antibody (1:200 in 2.5% normal goat serum; Thermo Fisher Scientific) for 1 h at room temperature. The cover slips were mounted with 4′,6-diamidino-2-phenylindole containing mounting solution (ImmunoBioscience, USA), and the images were then monitored using a fluorescence microscope (STED CW; Leica, Germany). Quantification of the overlapping area between mitotracker red fluorescent signals and green fluorescent signals of HA was performed by using Image J program.

Immunoprecipitation

COS7 cells were transfected with pcDNA-HA or pcDNA-HA-ACSL1 (250 ng) and pCMV-CPT1b-Myc (250 ng) for 24 h. Cell lysates were prepared using lysis buffer (20 mmol/

L Tris-HCl, pH 7.4, 1% NP-40, 10 mmol/L $Na_4P_2O_7$, 2 mmol/L Na_3VO_4, 100 mmol/L NaF, 5 mmol/L EDTA, 7 μg/ml leupeptin, 7 μg/ml aprotinin, and 1 mmol/L phenylmethysulfonyl fluoride [PMSF]). The cell lysates (500 μg) were used for immunoprecipitation with anti-HA antibody-coupled agarose beads (Roche, Switzerland) for 4 h at 4°C. The precipitates were washed five times and resuspended with 2× SDS-PAGE sampling buffer followed by heating. After removing agarose beads by centrifugation, the same amount of sample was subjected to SDS-PAGE and blotted with specific antibodies.

Mitochondria fractionation

The cells were homogenized in ice-cold mitochondria isolation buffer (250 mmol/L sucrose, 10 mmol/L Tris-HCl and 1 mmol/L EDTA) and then cell debris was removed by centrifugation (700 × *g*). The supernatant was centrifuged at 1,000 × *g* for 15 min to collect the nuclear fraction. The supernatant was centrifuged at 10,000 × *g* for 30 min to collect the mitochondrial fraction, with the supernatant being the cytosolic fraction. The pellets were washed with PBS and resuspended with mitochondria isolation buffer, then incubated with proteinase K (20 μg/ml) for 15 min. Reactions were stopped by addition of 1 mmol/L PMSF.

Acyl-CoA synthetase activity assay

Total acyl-CoA synthase activity was measured by acyl-CoA synthetase (ACS) assay kit (Abcam, USA). C2C12 myotubes were infected with Ad-GFP, Ad-HA-ACSL1wt, or Ad-ACSL1mt (100 moi) for 24 h, and then homogenized in 100 μl Ice-cold ACS assay buffer. ACS activity was measured following the manufacture's protocol, and the H_2O_2 production rate was normalized by the amount of proteins.

Measurement of fatty acid oxidation

C2C12 myotubes were homogenized in ice-cold mitochondria isolation buffer. The lysates were incubated with 0.2 mmol/L [1-^{14}C] palmitate for 2 h. The $^{14}CO_2$ and ^{14}C-labeled acid-soluble metabolites were quantified using a liquid scintillation counter. Each radioactivity reading was normalized using the protein amount of each sample.

TAG and DAG contents

C2C12 myotubes were harvested in PBS containing magnesium and calcium, and the cell pellets were resuspended with 200 μl of the assay buffer of Triglyceride Colorimetric assay Kit (Cayman, USA), and TG content of the cells was measured following the manufacture's instruction. To measure DAG contents, cell pellets in PBS were sonicated, and then DAG were separated by methanol/chloroform extractions followed by drying under a freeze speedvac dryer overnight. The dried sample was resuspended with 100 μl assay buffer of Diacylglycerol Assay Kit (Abcam), and DAG content was measured. The cellular TG and DAG contents were normalized by protein amounts of the cells.

RNA preparation and quantitative polymerase chain reaction (qPCR)

Total RNA was extracted using TRIzol reagent (Invitrogen) according to the manufacturer's instructions. Real-time qPCR was performed using SYBR Premix Ex Taq reagents (Takara, Japan) and a 7500 real-time PCR system (Applied Biosystems, USA). Pairs of real-time PCR primers were as follows: *Acsl1* primers, 5′-ctggttgctgcctgagcttg-3′ and 5′-ttgccccttcacacacacc-3′; *Acsl3* primers, 5′-gccagaaaccaaaggccaac-3′ and 5′-gaacaatggctggacctccc-3′; *Acsl4* primers, 5′-ttcgagaagctgcaaatgcc-3′ and 5′-taccaaaccagtctcggggg-3′; *Acsl5* primers, 5′-ggaaaagggcctcacaccag-3′ and 5′-ctccgcatcatgcaggata-3′; *Acsl6* primers, 5′-cttcttcttggtgtcggggg-3′ and 5′-gaaaaactggcccaagtccg-3′; *Cpt1b* primers, 5′-aagtgtaggaccagccccga-3′ and 5′-tgcggactcgttggtacagg-3′

Western blot analysis

Antibodies against ACSL1, HA, and enolase (Santa Cruz Biotechnology); Glyceraldehyde 3-phosphate dehydrogenase (GAPDH), and γ-tubulin (Merck, USA); Myc, pAKT, and AKT (Cell Signaling Technology, USA); and prohibitin (NeoMarkers, USA) were used. Bands were visualized using an Enhanced Chemiluminescence kit (Thermo Fisher Scientific) and Amersham Imager 680 Blot and Gel Imagers (GE Healthcare Life Sciences, USA).

Statistical analysis

Statistical analysis of the data was conducted using Prism 8 (GraphPad Software, USA). Student's *t*-test and ANOVA were used to measure the differences between two mean values. Data were expressed as mean ± SEM, and data with a *P* value less than 0.05 were denoted as statistically significant.

RESULTS

The N-terminal region of ACSL1 is necessary for docking of ACSL1 on mitochondria in COS7 cells

When aligning amino acid sequences of ACSL isoforms, the N-terminal amino acid sequences of each ACSL isoform (for example, amino acids 1 to 100 of ACSL1) were totally different from those of other isoforms, but the remaining parts of the isoforms were highly conserved (Fig. 1A). We hypothesized that the N-terminal region of ACSL1 was necessary for ACSL1 to be located on mitochondria. To confirm this hypothesis, we generated an expression vector encoding the N-terminal 100 amino acid-truncated form of ACSL1 (HA-ACSL1mt) (Fig. 1A). Expressions of the wild type (HA-ACSL-1wt) and the mutant form (HA-ACSL1mt) of ACSL1 were confirmed by western blot analysis after transfection of the constructs into COS7 cells (Fig. 1B). Their cellular distribution was detected by immunofluorescent analysis using an HA antibody. The majority of HA-ACSL1wt (82% of total HA-ACSL1wt) was co-localized with mitotracker, a mitochondria-selective probe, whereas only a small degree of HA-ACSL1mt (5.2% of total HA-ACSL1mt) was co-localized with mitotracker (Figs. 1C and 1D). These results suggest that ACSL1 is located in mitochondria via the N-terminal 100 amino acid region.

ACSL1 adjoins the outer membrane of mitochondria in C2C12 myotubes

Adenovirus harboring the expression systems for HA-ACSL-1wt or HA-ACSL1mt were infected into C2C12 myotubes,

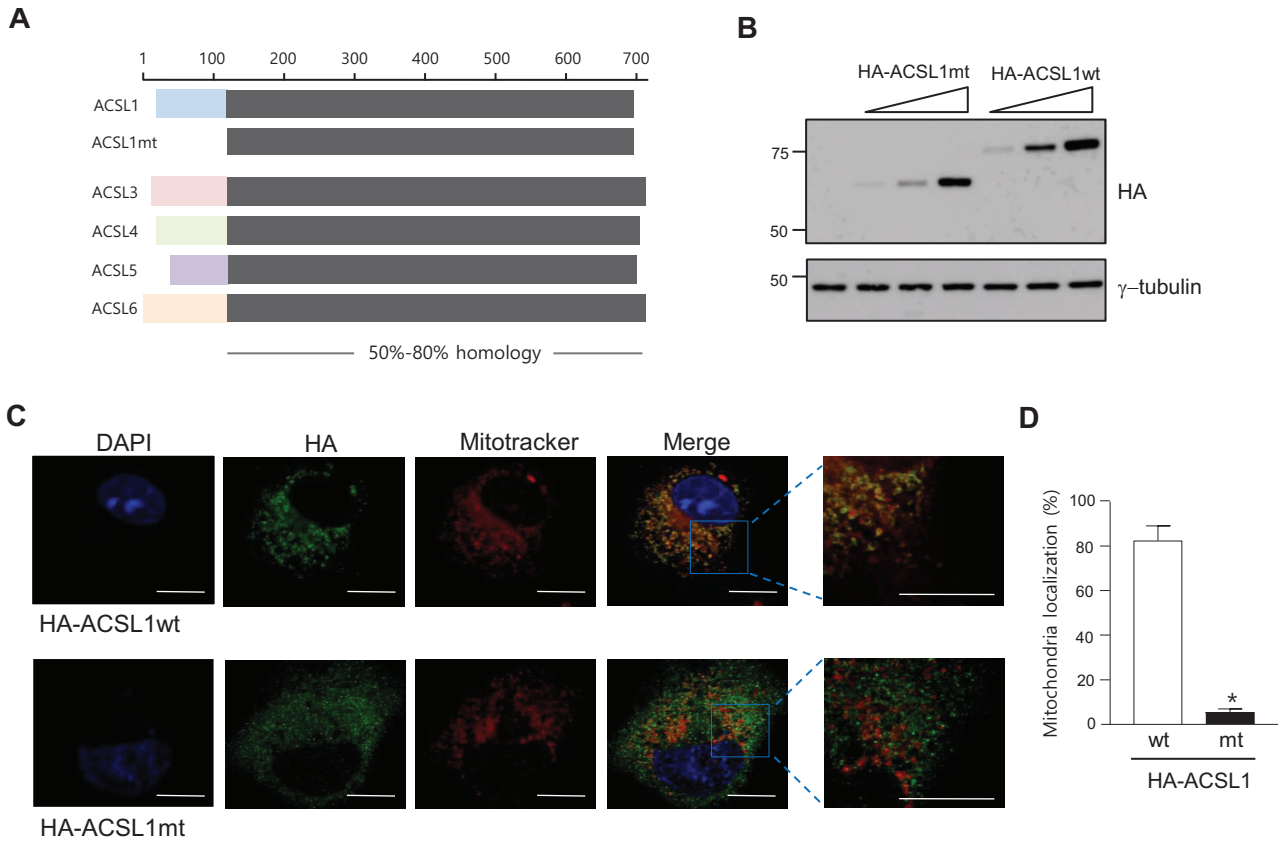

Fig. 1. Structure of ACSLs and the ACSL1 mutant. (A) Sequence comparison of mouse ACSL family members and the N-terminal-deleted ACSL1 mutant (ACSL1mt). (B) ACSL1 expression was detected by western blot analysis after transfection of pc-HA-ACSL1 wild type (wt) and pc-HA-ACSL1 mutant (mt) into COS7 cells. (C) Immunofluorescence micrographs after transfection of pc-HA-ACSL1wt or pc-HA-ACSL1mt in COS7 cells. Scale bars = 10 μm. (D) The ratio of mitochondrial co-localized HA-ACSL1 to total HA-ACSL1 was measured. n = 4, $*P < 0.05$ vs HA-ACSL1wt, by *t*-test.

and then the cellular distributions were determined. ACSL-1wt, but not ACSL1mt, was located at mitochondria, which was confirmed by immunofluorescence and cellular organelle fractionation (Figs. 2A and 2B). In addition, protease K treatment of the mitochondrial fraction removed the ACSL1wt western blot bands, indicating that ACSL1 localized to the outer membranes of mitochondria.

It has been reported that ACSL1 is located at ER as well as mitochondria in hepatocytes, and overexpressed ACSL1 is mainly placed on ER (Li et al., 2006). We tested whether the N-terminal deletion also affects ACSL1 localization on ER in hepatocytes. Both HA-ACSL1wt and HA-ACSL1mt overexpressed by the adeno virus system were located at the ER, while a little portion of ACSL1wt, but not ACSL1mt, showed colocalization with mitotracker (Fig. 2C). These results suggest that the N-terminal region of ACSL1 is important for targeting to mitochondria but not to ER.

ACSL1 interacts with CPT1b on the outer membranes of mitochondria

Because ACSL1 does not contain the mitochondrial targeting signal sequence, mitochondrial targeting might be mediated by interaction with a protein(s) embedded in the mitochondrial outer membrane. We tested whether CPT1b knockdown affected cellular ACSL1 localization. When CPT1b was knocked-down by transfection of siRNAs against CPT1b in C2C12 myotubes, ACSL1 was no longer located on mitochondria (Fig. 3A). Using the same conditions, the mRNA levels of CPT1b were decreased to ~30% (Fig. 3B). These results suggested that CPT1b was a major mitochondrial protein that interacted with ACSL1 in C2C12 myotubes. To confirm a direct interaction between ACSL1 and CPT1b, co-immunoprecipitation was performed after transfection of expression vectors for HA-ACSL1 and Myc-CPT1b into COS7 cells. Myc-CPT1b co-immunoprecipitated with HA-ACSL1wt but not with HA-ACSL1mt (Fig. 3C), showing that ACSL1 interacted with CPT1b, and that this interaction required its N-terminal region.

ACSL1 plays an important role in palmitate-induced FAO in myotubes

We have shown that exposure of C2C12 myotubes to high levels of palmitate increased FAO by an increase in the expression of FAO-related proteins such as CPT1b and ACSL1 (Koo et al., 2015). In the present study, we tested whether palmitate treatment affected the expressions of other ACSL

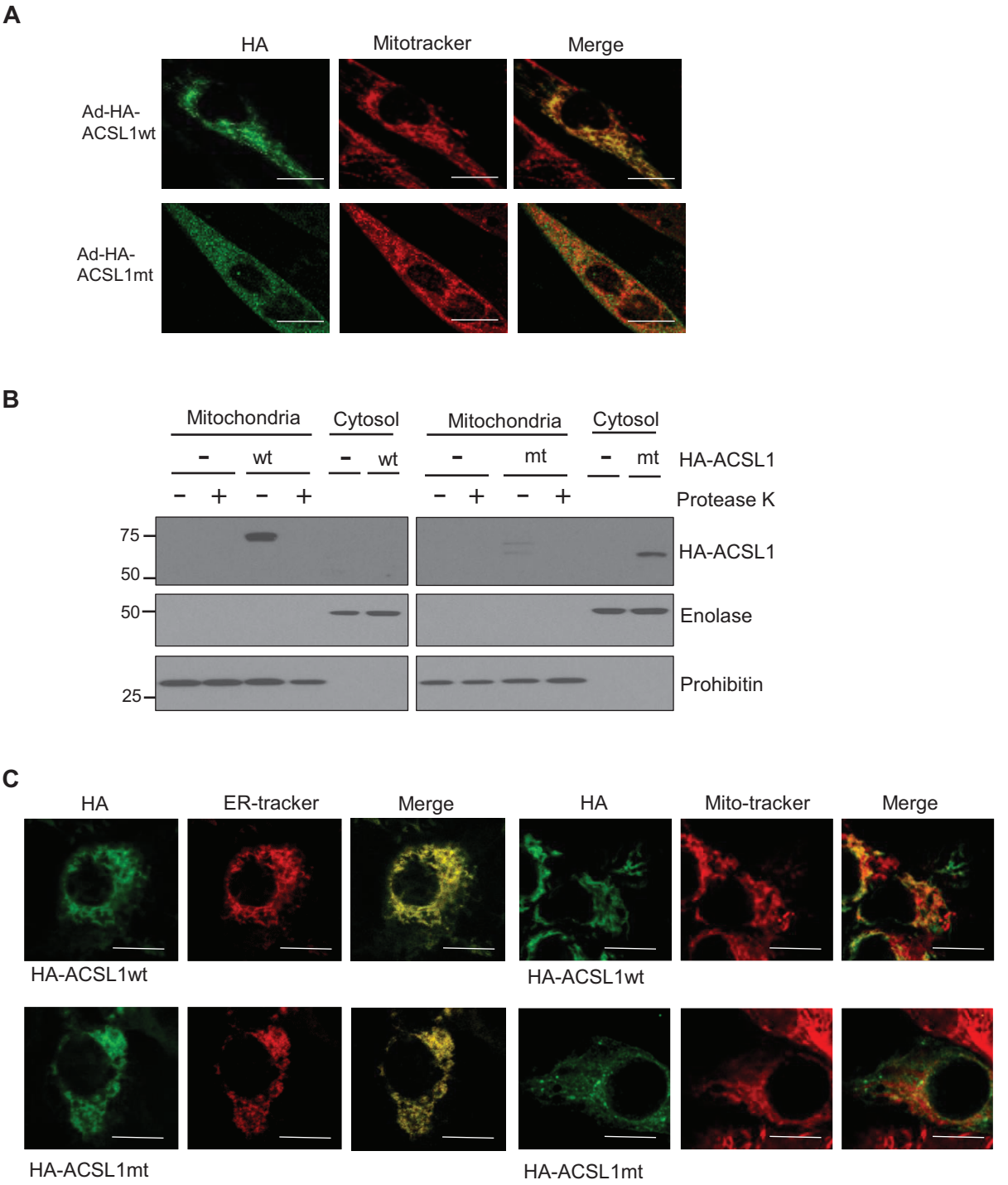

Fig. 2. Intracellular distribution of wild type ACSL1 (ACSL1wt) and mutant ACSL1 (ACSL1mt) in C2C12 myotubes. (A) Immunofluorescence micrographic analysis was performed after C2C12 myotubes were infected with Ad-HA-ACSL1wt or Ad-HA-ACSL1mt. Scale bars = 10 μm. (B) Subcellular fractionation was performed after infection with Ad-HA-ACSL1wt or Ad-HA-ACSL1mt into C2C12 myotubes. One half of the mitochondrial fraction was treated with protease K. Mitochondrial fractionation was confirmed by western blotting with antibodies against enolase (cytosol) and prohibitin (mitochondria). (C) Immunofluorescence micrographic analysis was performed after HepG2 cells were infected with Ad-HA-ACSL1wt or Ad-HA-ACSL1mt. Scale bars = 10 μm.

isoforms in addition to ACSL1 in C2C12 myotubes. We found that basal mRNA levels of ACSL3 and ACSL4 were relatively high in C2C12 myotubes, but only ACSL1 expression was significantly increased by palmitate treatment (Fig. 4A). We next examined the effect of ACSL1 knockdown on FAO in C2C12 myotubes. ACSL1 and ACSL3 transcripts were decreased

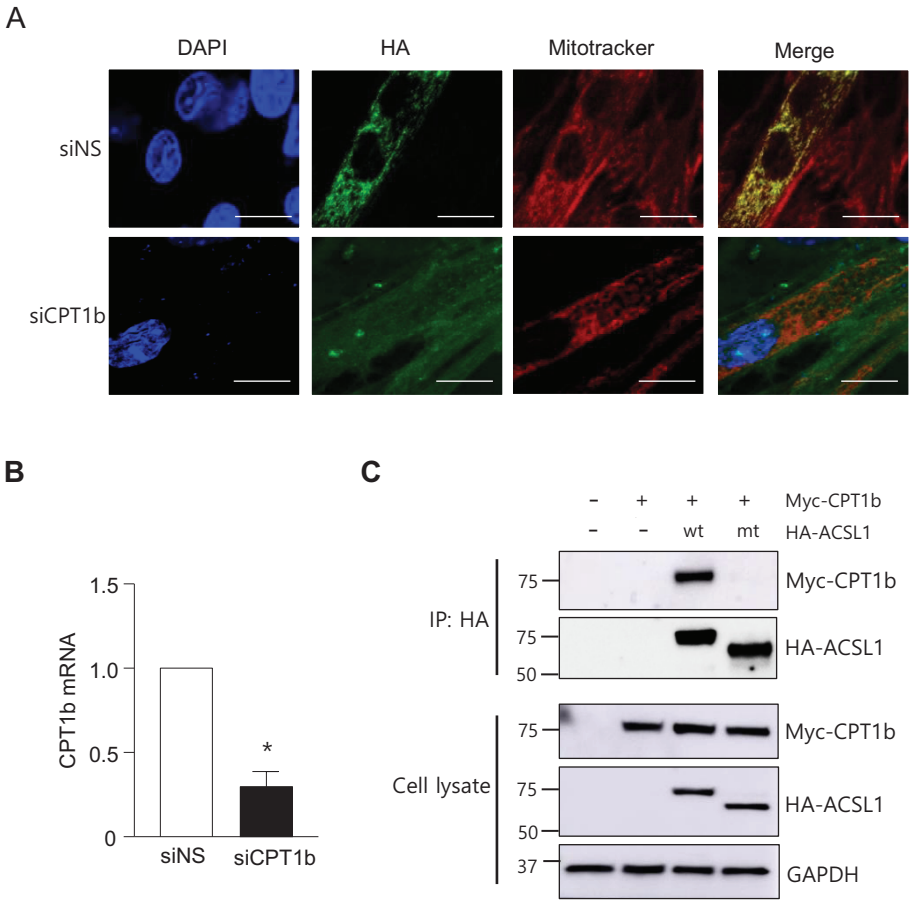

Fig. 3. ACSL1 interacts with a mitochondrial protein CPT1b in myotubes. (A) Immunofluorescence micrographs were conducted after C2C12 myotubes were treated with siNS (nonspecific) or siCPT1b for 48h. Scale bars = 10 μm. (B) Relative mRNA levels of CPT1b after treatment with siCPT1b in myotubes. n = 3, $*P < 0.05$ vs control, by *t*-test. (C) COS7 cells were co-transfected with pc-HA-ACSL1wt or pc-HA-ACSL1mt and pCMV-CPT1b-Myc. Immunoprecipitation (IP) was conducted with an HA antibody, and then western blotting was performed with HA or Myc antibodies.

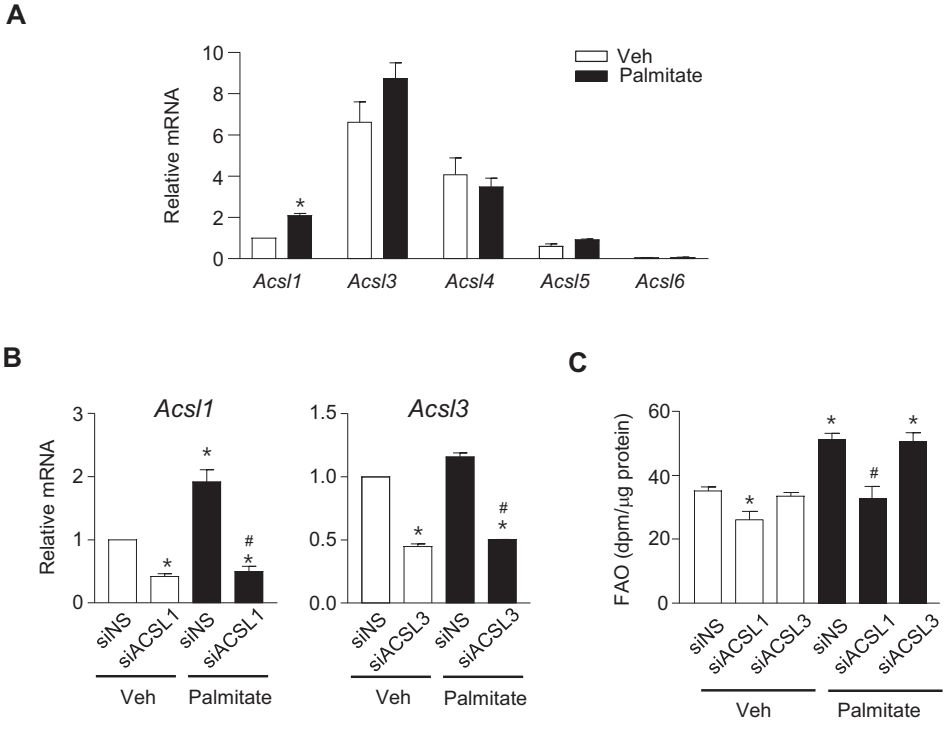

Fig. 4. ACSL1 mainly contributes to palmitate-induced FAO. (A) C2C12 myotubes were treated with 500 μmol/L palmitate for 24 h and relative mRNA levels of ACSL isoforms were determined using qPCR. The ACSL1 mRNA level of untreated cells (Veh) was set to 1, and others were expressed as its relative values. Data are expressed as the mean ± SEM, n = 3, $*P < 0.05$ vs Veh, by *t*-test. (B and C) C2C12 myotubes were transfected with siRNAs against ACSL1 and ACSL3 or siNS for 24 h and then treated with palmitate for 24 h. The mRNA levels of ACSLs (B) and FAO (C) were then determined. Data are expressed as mean ± SEM, n = 3, $*P < 0.05$ vs siNS/Veh, $^{\#}P < 0.05$ vs siNS/Palmitate, by ANOVA.

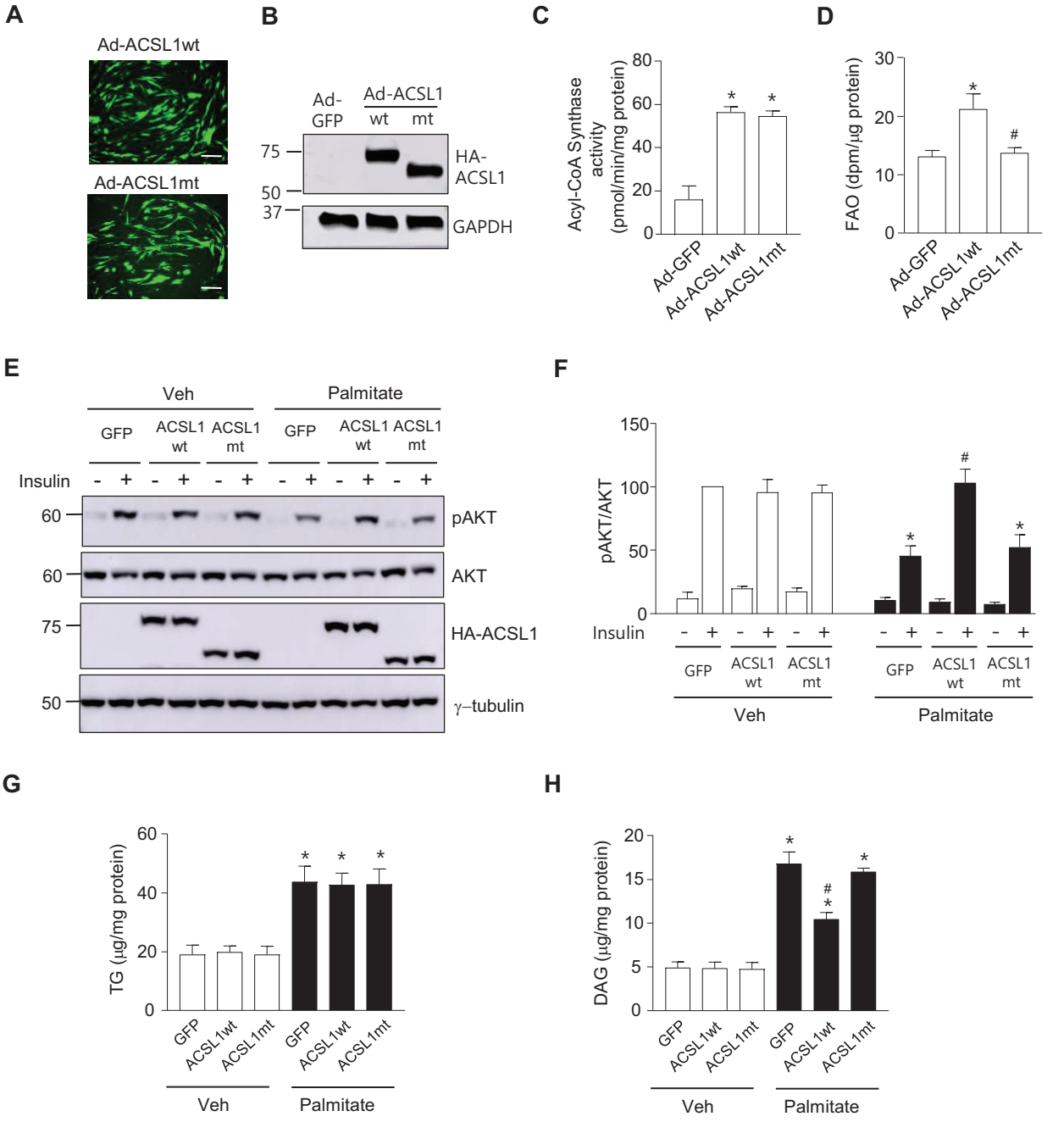

Fig. 5. ACSL1 overexpression ameliorates palmitate-induced insulin resistance. (A-D) Acyl CoA Synthase activity and FAO were measured after myotubes were infected with Ad-HA-ACSL1wt, Ad-HA-ACSL1mt or Ad-GFP (control) (100 moi) for 24 h. Viral infection was compared by detecting green fluorescent protein (GFP) expression, Scale bars = 100 μm (A), and expression of HA-ACSL1wt and HA-ACSL1mt was confirmed by western blotting (B). (C) Acyl-CoA synthase activity was measured, and H_2O_2 production rates were normalized by the amount of proteins in the cell lysates. Data are expressed as mean ± SEM, n = 3, $*P < 0.05$ vs Ad-GFP, by ANOVA. (D) FAO rates were measured. Data are expressed as mean ± SEM, n = 4, $*P < 0.05$ vs Ad-GFP, $^{\#}P < 0.05$ vs Ad-ACSL1wt, by ANOVA. (E and F) C2C12 myotubes were infected with Ad-HA-ACSL1wt, Ad-HA-ACSL1mt, or Ad-GFP (100 moi) for 24 h followed by palmitate (250 μmol/L) treatment for another 24 h, then stimulated with or without insulin (100 nmol/L) for 30 min. (E) Western blot analyses were performed with specific antibodies against pAKT (Ser473), AKT, HA, or γ-tubulin. (F) The ratio of pAKT to total AKT in the western blots was measured. The value of insulin stimulated pAKT/AKT of Ad-GFP-infected without palmitate-treated cells was set to 100, and the others were expressed as its relative values. Data are expressed as mean ± SEM, n = 3, $*P < 0.05$ vs Ad-GFP with insulin/Veh, $^{\#}P < 0.05$ vs Ad-GFP with insulin/palmitate, by ANOVA. (G and H) C2C12 myotubes were infected with Ad-HA-ACSL1wt, Ad-HA-ACSL1mt, or Ad-GFP (100 moi) for 24 h, and then intracellular TG (G) and DAG (H) levels were measured. Data are expressed as mean ± SEM, n = 5 (TG), n = 3 (DAG), $*P < 0.05$ vs Veh, $^{\#}P < 0.05$ vs Ad-GFP/Palmitate, by ANOVA.

by ~60% after transfection of siRNAs specific to ACSL1 (siACSL1) or ACSL3 (siACSL3) (Fig. 4B). FAO during the basal state decreased after ACSL1 knockdown. Furthermore, the palmitate-induced FAO increase disappeared after ACSL1 knockdown. In contrast, ACSL3 knockdown did not affect FAO, regardless of palmitate treatment (Fig. 4C). These results suggested that increased ACSL1 expression was important for palmitate-induced FAO in myotubes.

ACSL1 overexpression increases FAO and ameliorates palmitate-induced insulin resistance in C2C12 myotubes

Although ACSL1 plays a crucial role in linking free fatty acids to the mitochondrial β-oxidation pathway in various cell types, ACSL1 overexpression has not been shown to increase FAO in hepatocytes or adipocytes (Li et al., 2006; Zhao et al., 2020). We therefore examined whether ACSL1 overexpression affected FAO in C2C12 myotubes. C2C12 myotubes were infected with Ad-ACSL1wt or Ad-ACSL1mt for 24 h. The degree of virus infection and the amount of overexpressed ACSL1wt or ACSL1mt proteins were similar between these two groups (Figs. 5A and 5B). To confirm whether ACSL1mt retained its enzyme activity, total acyl-CoA synthase activity of the cell lysate was measured after infection of Ad-ACSL1wt or Ad-ACSL1mt into C2C12 myotubes. Acyl-CoA synthase activity was increased by overexpression of ACSL1mt as well as ACSL1wt, and no difference was observed between ACSL1wt and ACSL1mt (Fig. 5C). In contrast, overexpression of ACSL1wt, but not ACSL1mt, increased FAO (Fig. 5D), suggesting that overexpressed ACSL1 promoted FAO in myotubes and mitochondrial targeting is important for ACSL1 to mediate the FAO increase.

We next tested whether ACSL1 overexpression ameliorated insulin resistance induced by palmitate in C2C12 myotubes. Insulin efficiently increased pAKT levels in ACSL1wt-overexpressed myotubes even after palmitate treatment. In contrast, insulin signaling was attenuated by palmitate in myotubes infected with Ad-GFP or Ad-ACSL1mt (Figs. 5E and 5F). Excess intracellular fatty acids are converted to deleterious fatty acid-derived lipids such as DAG and ceramide. Increase of intracellular DAG activates specific protein kinase C (PKC) isoforms, PKCθ or PKCε, which attenuate the insulin signaling pathway (Palomer et al., 2018). In contrast, TG is considered to be harmless because it is not a signaling lipid (Listenberger et al., 2003). Therefore, we measured the effects of ACSL1wt or ACSL1mt overexpression on TG and DAG levels in myotubes exposed to high level of palmitate. Intracellular TG levels were increased after palmitate treatment, but not affected by overexpression of either ACSL1wt or ACSL1mt (Fig. 5G). However, ACSL1wt, but not ACSL1mt, overexpression significantly attenuated the increase of intracellular DAG upon palmitate treatment, which might be due to the increased FAO by ACSL1wt (Fig. 5H). Ultimately, these results suggested that increases of FAO by ACSL1 overexpression prevented palmitate-induced insulin resistance in myotubes.

Taken together, our data showed that ACSL1 was located on mitochondria through the interaction of its N-terminal region with CPT1b in myotubes. In addition, overexpression of ACSL1 increased FAO in myotubes, which provided a protective effect on palmitate-induced insulin resistance.

DISCUSSION

Mitochondrial localization of ACSL1 has been reported in various cell types; however, ACSL1 does not have mitochondrial targeting sequences. It is therefore possible that ACSL1 targets to mitochondria through an interaction with a protein(s) embedded on the outer membrane. In the present study, we found that ACSL1 was localized to mitochondria through the direct interaction with CPT1b in C2C12 myotubes, and that the N-terminal 100 amino acids of ACSL1 were necessary for this interaction. Five ACSL isoforms (ACSL1, 3, 4, 5, and 6) have distinct N-terminal domains, with the remaining parts having substantially conserved amino acid sequences. Our results suggested that the N-terminal regions of ACSL isoforms played important roles in determining their intracellular distribution and interactions with other proteins.

A previous study reported that ACSL1 interacted with several proteins on the mitochondria of hepatocytes and that CPT1a was one of the interacting proteins (Young et al., 2018). In contrast, our results showed that CPT1b was a major mitochondrial protein interacting with ACSL1 in myotubes, because knockdown of CPT1b removed most of the mitochondrial targeting of ACSL1 (Fig. 3A). There is approximately 70% homology between CPT1a and CPT1b, therefore it will be interesting to compare binding affinities of ACSL1 with two different CPT1 members. CPT1 on the outer membrane of mitochondria converts Acyl-CoA to acyl-carnitine, which then enters into mitochondria. The interaction between ACSL1 and CPT1b therefore provides an efficient trigger of FAO in myotubes.

The effects of ectopic expression of ACSL1 on lipid metabolism have been studied in various cell types and tissues. ACSL1 overexpression in hepatocytes increases cellular accumulation of TG, but does not affect FAO (Parkes et al., 2006). It is well-known that ACSL1 is located not only on mitochondria but also on ER in hepatocytes, and overexpressed ACSL1 targets to the ER but not to mitochondria (Li et al., 2006). In addition, overexpression of ACSL1 in adipocytes increases fatty acid uptake and synthesis of polyunsaturated fatty acids without any increase of FAO (Zhan et al., 2012; Zhao et al., 2020). In contrast, we showed that ACSL1 overexpression in C2C12 myotubes increased FAO, with localization of overexpressed ACSL1 on mitochondria. These results suggested that targeting of ectopically expressed ACSL1 to mitochondria was important in increasing FAO.

Our data also showed that palmitate treatment of myotubes increased the expression of ACSL1, without any change in the expressions of other ACSL members (Fig. 4A), which is assumed to be compensatory action to overcome lipotoxicity. It is well-known that overexpression of CPT1b increases FAO in skeletal myotubes (Sebastian et al., 2009). In addition, we showed that ectopic expression of ACSL1 ameliorated insulin resistance induced by palmitate in myotubes. Therefore, the increase of ACSL1/CPT1b-mediated FAO in skeletal muscles could ameliorate insulin resistance in obesity and related metabolic disorders.

ACKNOWLEDGMENTS
This research was supported by Basic Science research Program through the National Research Foundation of Korea (NRF) funded by the Ministry of education (NRF-2019R1A2C3009517) (NRF-2019R1A2C1008633).

AUTHOR CONTRIBUTIONS
J.N. and J.S.L. performed the experiments. S.A.L. and D.S.L. gave technical support and analyzed the data. K.S.P. and S.S.C. conceived and supervised the study. J.N., S.S.C., S.A.L., and K.S.P. wrote and edited the manuscript.

CONFLICT OF INTEREST
The authors have no potential conflicts of interest to disclose.

ORCID
Jinyan Nan https://orcid.org/0000-0001-9507-9943
Ji Seon Lee https://orcid.org/0000-0002-9769-7726
Seung-Ah Lee https://orcid.org/0000-0002-9192-2849
Dong-Sup Lee https://orcid.org/0000-0001-8312-2705
Kyong Soo Park https://orcid.org/0000-0003-3597-342X
Sung Soo Chung https://orcid.org/0000-0002-6017-0525

REFERENCES
Badin, P.M., Langin, D., and Moro, C. (2013). Dynamics of skeletal muscle lipid pools. Trends Endocrinol. Metab. *24*, 607-615.

Bowman, T.A., O'Keeffe, K.R., D'Aquila, T., Yan, Q.W., Griffin, J.D., Killion, E.A., Salter, D.M., Mashek, D.G., Buhman, K.K., and Greenberg, A.S. (2016). Acyl CoA synthetase 5 (ACSL5) ablation in mice increases energy expenditure and insulin sensitivity and delays fat absorption. Mol. Metab. *5*, 210-220.

Bruce, C.R., Hoy, A.J., Turner, N., Watt, M.J., Allen, T.L., Carpenter, K., Cooney, G.J., Febbraio, M.A., and Kraegen, E.W. (2009). Overexpression of carnitine palmitoyltransferase-1 in skeletal muscle is sufficient to enhance fatty acid oxidation and improve high-fat diet-induced insulin resistance. Diabetes *58*, 550-558.

Bu, S.Y., Mashek, M.T., and Mashek, D.G. (2009). Suppression of long chain acyl-CoA synthetase 3 decreases hepatic de novo fatty acid synthesis through decreased transcriptional activity. J. Biol. Chem. *284*, 30474-30483.

Chaurasia, B. and Summers, S.A. (2015). Ceramides - lipotoxic inducers of metabolic disorders. Trends Endocrinol. Metab. *26*, 538-550.

Coll, T., Eyre, E., Rodriguez-Calvo, R., Palomer, X., Sanchez, R.M., Merlos, M., Laguna, J.C., and Vazquez-Carrera, M. (2008). Oleate reverses palmitate-induced insulin resistance and inflammation in skeletal muscle cells. J. Biol. Chem. *283*, 11107-11116.

Cooper, D.E., Young, P.A., Klett, E.L., and Coleman, R.A. (2015). Physiological consequences of compartmentalized acyl-CoA metabolism. J. Biol. Chem. *290*, 20023-20031.

Czech, M.P. (2017). Insulin action and resistance in obesity and type 2 diabetes. Nat. Med. *23*, 804-814.

Ellis, J.M., Li, L.O., Wu, P.C., Koves, T.R., Ilkayeva, O., Stevens, R.D., Watkins, S.M., Muoio, D.M., and Coleman, R.A. (2010). Adipose acyl-CoA synthetase-1 directs fatty acids toward beta-oxidation and is required for cold thermogenesis. Cell Metab. *12*, 53-64.

Gargiulo, C.E., Stuhlsatz-Krouper, S.M., and Schaffer, J.E. (1999). Localization of adipocyte long-chain fatty acyl-CoA synthetase at the plasma membrane. J. Lipid Res. *40*, 881-892.

Grevengoed, T.J., Cooper, D.E., Young, P.A., Ellis, J.M., and Coleman, R.A. (2015). Loss of long-chain acyl-CoA synthetase isoform 1 impairs cardiac autophagy and mitochondrial structure through mechanistic target of rapamycin complex 1 activation. FASEB J. *29*, 4641-4653.

Henique, C., Mansouri, A., Fumey, G., Lenoir, V., Girard, J., Bouillaud, F., Prip-Buus, C., and Cohen, I. (2010). Increased mitochondrial fatty acid oxidation is sufficient to protect skeletal muscle cells from palmitate-induced apoptosis. J. Biol. Chem. *285*, 36818-36827.

Kelley, D.E. and Mandarino, L.J. (2000). Fuel selection in human skeletal muscle in insulin resistance: a reexamination. Diabetes *49*, 677-683.

Koo, Y.D., Choi, J.W., Kim, M., Chae, S., Ahn, B.Y., Kim, M., Oh, B.C., Hwang, D., Seol, J.H., Kim, Y.B., et al. (2015). SUMO-specific protease 2 (SENP2) is an important regulator of fatty acid metabolism in skeletal muscle. Diabetes *64*, 2420-2431.

Koves, T.R., Ussher, J.R., Noland, R.C., Slentz, D., Mosedale, M., Ilkayeva, O., Bain, J., Stevens, R., Dyck, J.R., Newgard, C.B., et al. (2008). Mitochondrial overload and incomplete fatty acid oxidation contribute to skeletal muscle insulin resistance. Cell Metab. *7*, 45-56.

Li, L.O., Ellis, J.M., Paich, H.A., Wang, S., Gong, N., Altshuller, G., Thresher, R.J., Koves, T.R., Watkins, S.M., Muoio, D.M., et al. (2009). Liver-specific loss of long chain acyl-CoA synthetase-1 decreases triacylglycerol synthesis and beta-oxidation and alters phospholipid fatty acid composition. J. Biol. Chem. *284*, 27816-27826.

Li, L.O., Grevengoed, T.J., Paul, D.S., Ilkayeva, O., Koves, T.R., Pascual, F., Newgard, C.B., Muoio, D.M., and Coleman, R.A. (2015). Compartmentalized acyl-CoA metabolism in skeletal muscle regulates systemic glucose homeostasis. Diabetes *64*, 23-35.

Li, L.O., Mashek, D.G., An, J., Doughman, S.D., Newgard, C.B., and Coleman, R.A. (2006). Overexpression of rat long chain acyl-coa synthetase 1 alters fatty acid metabolism in rat primary hepatocytes. J. Biol. Chem. *281*, 37246-37255.

Listenberger, L.L., Han, X., Lewis, S.E., Cases, S., Farese, R.V., Jr., Ory, D.S., and Schaffer, J.E. (2003). Triglyceride accumulation protects against fatty acid-induced lipotoxicity. Proc. Natl. Acad. Sci. U. S. A. *100*, 3077-3082.

Mannaerts, G.P., Van Veldhoven, P., Van Broekhoven, A., Vandebroek, G., and Debeer, L.J. (1982). Evidence that peroxisomal acyl-CoA synthetase is located at the cytoplasmic side of the peroxisomal membrane. Biochem. J. *204*, 17-23.

Mashek, D.G., Li, L.O., and Coleman, R.A. (2006). Rat long-chain acyl-CoA synthetase mRNA, protein, and activity vary in tissue distribution and in response to diet. J. Lipid Res. *47*, 2004-2010.

Palomer, X., Pizarro-Delgado, J., Barroso, E., and Vazquez-Carrera, M. (2018). Palmitic and oleic acid: the yin and yang of fatty acids in type 2 diabetes mellitus. Trends Endocrinol. Metab. *29*, 178-190.

Parkes, H.A., Preston, E., Wilks, D., Ballesteros, M., Carpenter, L., Wood, L., Kraegen, E.W., Furler, S.M., and Cooney, G.J. (2006). Overexpression of acyl-CoA synthetase-1 increases lipid deposition in hepatic (HepG2) cells and rodent liver in vivo. Am. J. Physiol. Endocrinol. Metab. *291*, E737-E744.

Sebastian, D., Guitart, M., Garcia-Martinez, C., Mauvezin, C., Orellana-Gavalda, J.M., Serra, D., Gomez-Foix, A.M., Hegardt, F.G., and Asins, G. (2009). Novel role of FATP1 in mitochondrial fatty acid oxidation in skeletal muscle cells. J. Lipid Res. *50*, 1789-1799.

Sebastian, D., Herrero, L., Serra, D., Asins, G., and Hegardt, F.G. (2007). CPT I overexpression protects L6E9 muscle cells from fatty acid-induced insulin resistance. Am. J. Physiol. Endocrinol. Metab. *292*, E677-E686.

Soupene, E. and Kuypers, F.A. (2006). Multiple erythroid isoforms of human long-chain acyl-CoA synthetases are produced by switch of the fatty acid gate domains. BMC Mol. Biol. *7*, 21.

Soupene, E. and Kuypers, F.A. (2008). Mammalian long-chain acyl-CoA synthetases. Exp. Biol. Med. (Maywood) *233*, 507-521.

Teodoro, B.G., Sampaio, I.H., Bomfim, L.H., Queiroz, A.L., Silveira, L.R., Souza, A.O., Fernandes, A.M., Eberlin, M.N., Huang, T.Y., Zheng, D., et al.

(2017). Long-chain acyl-CoA synthetase 6 regulates lipid synthesis and mitochondrial oxidative capacity in human and rat skeletal muscle. J. Physiol. *595*, 677-693.

Young, P.A., Senkal, C.E., Suchanek, A.L., Grevengoed, T.J., Lin, D.D., Zhao, L., Crunk, A.E., Klett, E.L., Fullekrug, J., Obeid, L.M., et al. (2018). Long-chain acyl-CoA synthetase 1 interacts with key proteins that activate and direct fatty acids into niche hepatic pathways. J. Biol. Chem. *293*, 16724-16740.

Zhan, T., Poppelreuther, M., Ehehalt, R., and Fullekrug, J. (2012). Overexpressed FATP*1*, ACSVL4/FATP4 and ACSL1 increase the cellular fatty acid uptake of 3T3-L1 adipocytes but are localized on intracellular membranes. PLoS One *7*, e45087.

Zhao, L., Pascual, F., Bacudio, L., Suchanek, A.L., Young, P.A., Li, L.O., Martin, S.A., Camporez, J.P., Perry, R.J., Shulman, G.I., et al. (2019). Defective fatty acid oxidation in mice with muscle-specific acyl-CoA synthetase 1 deficiency increases amino acid use and impairs muscle function. J. Biol. Chem. *294*, 8819-8833.

Zhao, Z., Abbas Raza, S.H., Tian, H., Shi, B., Luo, Y., Wang, J., Liu, X., Li, S., Bai, Y., and Hu, J. (2020). Effects of overexpression of ACSL1 gene on the synthesis of unsaturated fatty acids in adipocytes of bovine. Arch. Biochem. Biophys. *695*, 108648.